*Article*

# A Novel High Isolation 4-Port Compact MIMO Antenna with DGS for 5G Applications

**Cem Güler [1,‡], Sena Esen Bayer Keskin [2*,‡]**

[1] Department of Airframe and Powerplant Maintenance, Kırklareli University, Kırklareli 39750, Turkey, cemguler@klu.edu.tr
[2] Electrical and Electronics Engineering Department, Kırklareli University, Kırklareli 39100, Turkey, senakeskin@klu.edu.tr
* Correspondence: senakeskin@klu.edu.tr
‡ These authors contributed equally to this work.

**Abstract:** This paper presents the design and realization of a simple and low-profile, 4-port Multiple-Input-Multiple-Output (MIMO) antenna operating in the mm-wave band supporting 5G communication technologies. As part of the design methodology, the initial stage involved the development of a conventional monopole patch antenna optimized for operation at 26 GHz, which is matched to 50 stepped feed line. Afterward, a square-shaped Defected Ground Structure (DGS) with semi-circles slots on the edges is placed on the ground to improve the isolation and the circular and rectangular slots are incorporated as DGS to optimize the antenna impedance bandwidth. Etching semi-circular shaped slots on the ground plane achieved more then 34.2 dB isolation in the 26 GHz operating band. In addition, an arrangement of four symmetrical radiating elements is positioned orthogonally to minimize the antenna's physical size and to improve the isolation. The proposed MIMO antenna overall dimension is 25  25 $mm^2$, which is printed on Rogers 5880 substrate with a width of 0.787 mm and $\varepsilon_r$ = 2.2. The proposed antenna covers the 5G mm-wave band with a 10 dB bandwidth ranging from 25.28 - 28.02 GHz, whereas the maximum gain attained for the purposed structure is 8.72 dBi. Moreover, the proposed design, simulated and measured with advantages such as high isolation, low ECC, simple and compact design, is a good candidate for usage areas such as smart devices, mobile phones, and sensors in 5G applications.

**Keywords:** 5G; MIMO; isolation; slot; ECC

## 1. Introduction

Wireless communication systems have become essential in various areas such as health, agriculture, finance, education, the Internet of Things, media, and entertainment [1–5]. Mobile communication generations must be updated approximately every ten years as the demand for faster and more reliable connections grows [6]. The latest generation of wireless communication systems, 5G technology, offers several advantages over previous generations, including higher data rates, reliable connections, and reduced latency in three different usage scenarios (eMBB, uRLLC, and mMTC) [7]. In addition, 5G technology can decrease energy consumption by up to 90% [8,9]. However, the use of a single antenna in the millimeter wave region, such as the 26 GHz band, results in signal quality degradation due to atmospheric conditions and path loss attenuation [10]. These challenges need to be addressed to ensure the optimal performance of wireless communication systems in the millimeter wave region. MIMO technology employs spatial multiplexing techniques that enable high data transfer rates while maintaining signal quality, even in challenging environments [11,12]. Using MIMO antennas provides the high data transmission rate that 5G technology is expected to offer using spatial multiplexing [13–15]. Nevertheless, in MIMO antenna design, since the antenna elements share a single dielectric layer, the mutual coupling between antenna elements caused by their close proximity in MIMO systems is a challenge that needs to be addressed [16,17]. EBG structures are commonly used in 5G millimeter wave applications to increase isolation between MIMO antenna elements by restricting the movement of surface current waves [18,19]. Studies have reported EBG

 doi:10.20944/preprints202305.1709.v1



structures providing isolation values of over 25 dB [20], with other studies achieving 23 dB isolation values between radiating antennas [21]. However, the complexity and production difficulties of EBG designs, low bandwidth, and low gain values have limited the use of this method. Decoupling networks (DNs) have been proposed to reduce mutual coupling between antenna elements, offering enhanced gain and reduced interference [22]. However, they also have significant drawbacks, requiring more space between radiating elements and potentially increasing power losses. In MIMO antenna systems, DNs have been shown to reduce mutual interaction between elements, achieving an isolation level of 20 dB [23]. Nonetheless, ensuring the stability of the DN is crucial, as any instability can severely impact the antenna's performance and bandwidth. Using parasitic elements (PE) can improve isolation levels [24]. An asymptotic structure to reduce the connection between antenna elements achieves an isolation value of 16.4 dB [25]. It is stated that using C-shaped parasitic elements between MIMO antenna elements improves mutual coupling by 8.58 dB to reduce the connection between antennas [26]. Although PE successfully improves the isolation level, adding PE between the elements causes a shift in the antenna's frequency and requires redesigning the antenna. Therefore, using different parasitic elements for antennas operating at different frequencies is impractical. Neutralization lines are preferred in MIMO antenna designs due to their ability to facilitate easy impedance matching. Using NL in a MIMO antenna designed using characteristic mode analysis results in an isolation value of 16 dB [27]. NL used in two and four-port MIMO antennas achieve an isolation value of over 22 dB and 23 dB, respectively [28]. The length of the NL, which is preferred at low frequencies, depends on the antenna frequency, and as the bandwidth increases, the length of the line also increases, causing additional cost problems. In addition, it is crucial to install NL correctly. More installation is needed to maintain the efficiency of the lines. Additionally, hybrid isolation development techniques emerge with the combined use of these methods. Various hybrid methods exist, such as the use of EBG and DGS together [29], L-shaped stubs, defective ground, and chip resistors used together [30], the use of the DGS method on the ground plane and epsilon-and-mu-near-zero-based metasurface superstrate [31], and the use of slot and parasitic element structures [32]. Also, various techniques have been employed to enhance the isolation levels in MIMO antennas by mitigating mutual coupling effects, such as the integration of vias [33], a zigzag-shaped slotted structure in the ground plane [34], a partially reflecting surface [35], a partial ground surface [36], a partial ground surface combined with metasurface [37], a slot in the ground plane [38–45], decoupling branches [46], and a stub in the ground plane [47]. The techniques for enhancing isolation used in prior research are known to be expensive and involve several processing steps. As antenna dimensions decrease in the millimeter waveband, producing complex designs becomes increasingly challenging. To address these difficulties, this article introduces a novel 4-port MIMO antenna design that operates in the millimeter waveband and exhibits a low profile, small size, wide bandwidth, and high isolation value compared to the studies in the literature. The incorporation of two rectangular slots in the ground plane, positioned immediately behind the junction of the transmission line and the patch as well as the circular slot integrated in the ground plane, facilitates coverage of the frequency band spectrum designated for 5G millimeter-wave applications by optimizing the center frequency within the bandwidth. In addition, proposed design features orthogonally placed radiating patches that minimize the physical size of the antenna and enhance isolation. In addition, a semicircular DGS is incorporated at the edges of the ground plane to further improve isolation between antenna elements. This is due to the fact that the curved geometry of the semi-circular slots help to redirect the coupling effect away from the antenna elements and reduce the coupling between adjacent antenna elements, resulting in a stronger isolation between the ports. Overall, the proposed design employs the defected ground structure to reduce the envelope correlation coefficient (ECC), a critical parameter for MIMO antennas. The proposed antenna design is cost-effective, easy to manufacture, and a good candidate for use in 5G systems with improved isolation levels.

 doi:10.20944/preprints202305.1709.v1



## 2. Proposed Antenna Design

The usage of MIMO antennas in mm-wave applications is particularly valuable due to their low cost, low profile, and compact size. The appropriate design of 4-port MIMO antennas can result in strong isolation levels and optimal radiation characteristics, which are crucial for achieving high-performance wireless communication systems. The proposed antenna is designed with a stepped line feed, rectangular and circular slots implemented as defected ground structure for achieving wider bandwidth, in addition to optimal radiation characteristics. Moreover, it has been determined that the optimal radiation characteristics of the antenna can be achieved by incorporating semi-circular slots at the edges of the ground surface of the antenna elements, and by employing an orthogonal arrangement of the four antenna elements to achieve a strong isolation of at least 34.2 dB.

### *2.1. Design of the Unit Cell*

The unit cell of the proposed antenna comprises DGS and an antenna radiator, developed in three steps incorporating various geometrical shapes, such as rectangular and circular slots, the design steps of the unit cell illustrated in Figure 1. Figure 1a demonstrates the front view (radiating element) of the unit cell, while Figure 1b,c,d shows the back view design steps (ground plane) of the unit cell. In Step I, the conventional microstrip feed line is optimized with a stepped feed line structure, as illustrated in Figure 1a. This modification is aimed at enhancing the antenna's return loss and bandwidth characteristics. The stepped microstrip feed line design enables improved impedance matching and reduced signal reflection, thereby resulting in enhanced antenna performance. The ground surface of the unit cell in Step I is shown in Figure 1b. In Step II, two rectangular-shaped slots are etched into the ground plane, positioned directly behind the junction of the transmission line and the patch surface, creating DGS, as illustrated in Figure 1c. This modification effectively eliminates surface waves and results in improved performance of the antenna. The design with DGS enables a return loss of -30.93 dB to be achieved, as shown in Figure 1c. In Step III, the proposed ground plane design of the unit cell is presented, which includes the addition of a circular slot at the full-back alignment of the patch's top, as shown in Figure 1d. This modification enables the antenna to achieve a return loss of -38.65 dB, a bandwidth of 25.3 GHz to 27.6 GHz, and a center frequency of 26.26 GHz. By optimizing the center frequency within the bandwidth, the circular structure at the top of the patch helps to cover the frequency band spectrum designated for 5G mm-wave applications.

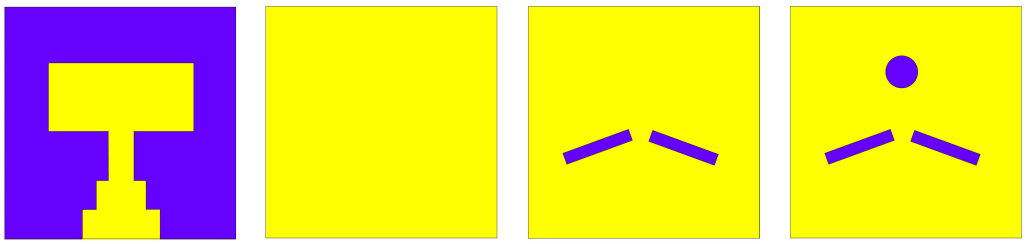


**Figure 1.** Design steps of the proposed unit cell. a) Front view of the unit cell, b) Back view of the unit cell – step I, c) Back view of the unit cell – step II, d) Back view of the unit cell – step III.

The unit cell of the proposed antenna resulting in the specific form illustrated in Figure 2. Figure 2a demonstrates the front view (radiating element), while Figure 2b shows the back view (ground plane), and Figure 2c displays the side view of the unit cell.

Preprints (www.preprints.org) | NOT PEER-REVIEWED | Posted: 24 May 2023 doi:10.20944/preprints202305.1709.v1



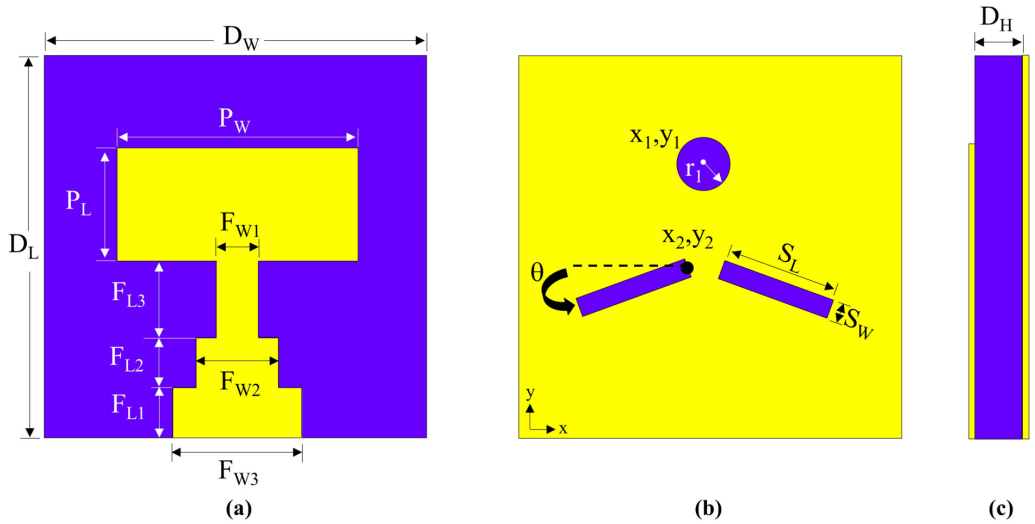


**Figure 2.** Design of the proposed unit cell of the MIMO antenna. a) Front view, b) Back view and c) Side view of the unit cell.

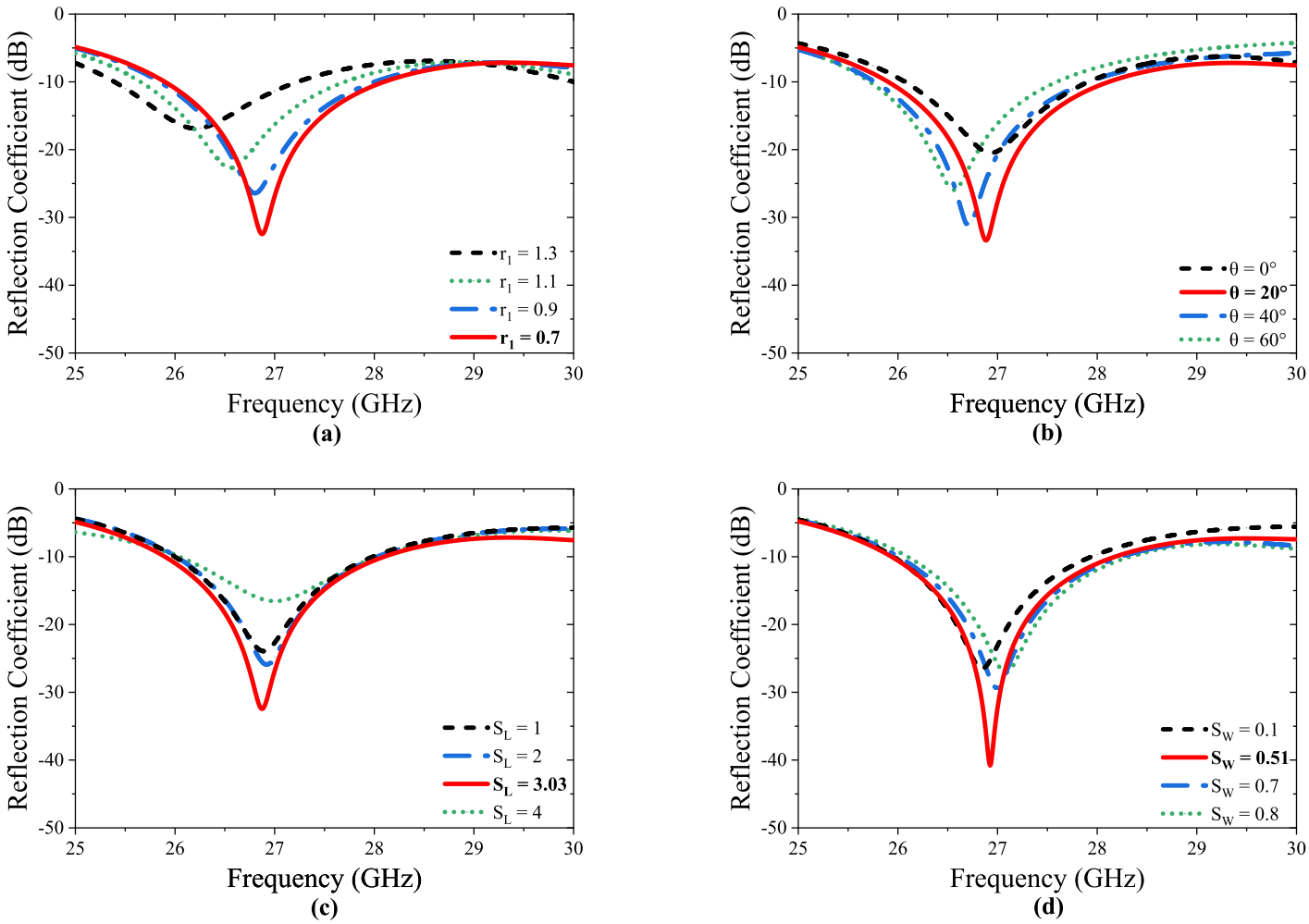


**Figure 3.** Parametric analysis of the unit cell: a) $r_1$, b) $\theta$, c) $S_L$ and d) $S_W$

The utilization of the DGS technique can significantly enhance the bandwidth of the unit cell in antenna design, thereby improving the overall performance across a wider range

Preprints (www.preprints.org) | NOT PEER-REVIEWED | Posted: 24 May 2023 doi:10.20944/preprints202305.1709.v1



of operating frequencies. Consequently, the introduction of a circular slot at the center of the ground plane, along with two rectangular slots positioned immediately behind the junction of the transmission line, facilitates the creation of the DGS. These slots indicate a defect in the ground plane, which affects the surface current distribution on the ground plane and, hence, the impedance and bandwidth of the antenna. Therefore, the diameters of the circular slot ($r_1$) and placement angle of rectangles ($\theta$), as well as the length ($S_L$) and width ($S_W$) of the rectangles, are optimized to improve the bandwidth, as shown in Figure 3. The optimized geometric dimensions of the proposed unit cell are presented in Table 1.

**Table 1.** Optimized geometric dimensions of the proposed unit cell of the MIMO antenna.

| Parameter | Value | Parameter | Value | Parameter | Value |
|---|---|---|---|---|---|
| $P_W$ | 6.301 | $F_{L1} = F_{L2}$ | 1.31 | $r_1$ | 0.7 |
| $P_L$ | 2.99 | $F_{L3}$ | 2.07 | $r_2$ | 1.28 |
| $F_{W1}$ | 1.05 | $x_1$,$y_1$ | (0.0 , 2.0) | $S_W$ | 3.03 |
| $F_{W2}$ | 2.06 | $x_2$,$y_2$ | (-0.3 , 0.71) | $S_L$ | 0.51 |
| $F_{W3}$ | 3.21 | $D_W = D_L$ | 10 | Theta | 20 |

Figure 4 shows reflection coefficient values corresponding to each antenna design step (Step I, Step II and Step III). The major resonance frequency of the MIMO system is at 26.3 GHz, and the return loss values ranged from -26.1 to -38.6 dB.

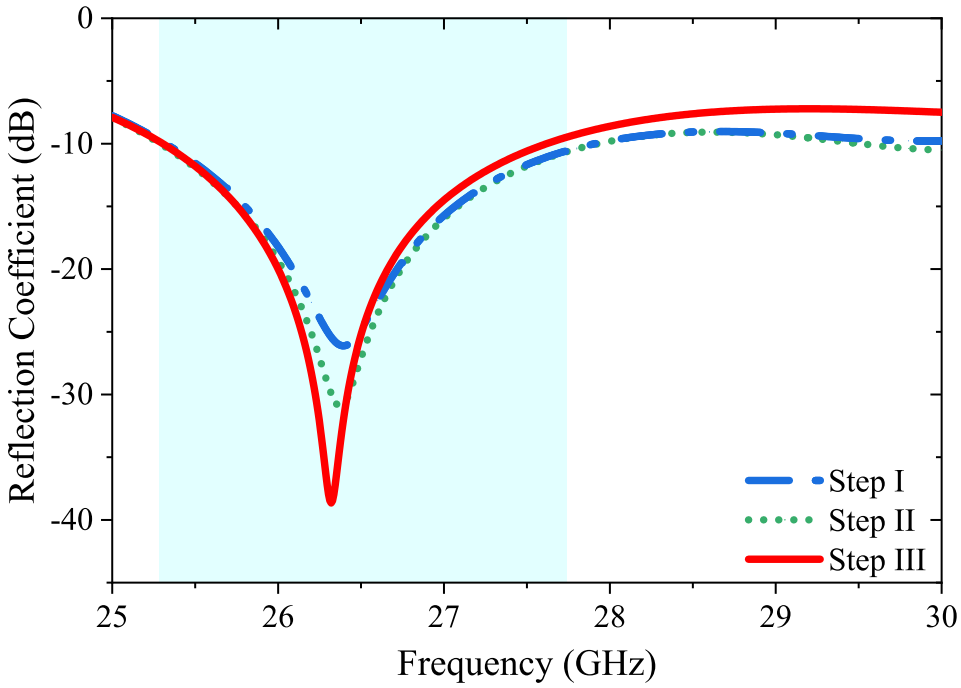


**Figure 4.** Reflection coefficient values for each antenna design step (Step I, Step II and Step III).

*2.2. 4-Port MIMO Antenna for 26 GHz 5G Application*

The developmental stages and a comprehensive 3D visualization of the physical structure of the 4-port MIMO antenna are presented in Figure 5. The DGS can also help to reduce the surface waves that propagate along the ground plane, which can improve the radiation efficiency of the antenna. Therefore, by introducing semi-circular slots at the edges of the ground surface as shown in Figure 5c, the geometry of the ground plane is effectively modified, which can affect the coupling between the antenna elements. Hence,

Preprints (www.preprints.org) | NOT PEER-REVIEWED | Posted: 24 May 2023 doi:10.20944/preprints202305.1709.v1



the diameter ($r_2$) of the semicircular slots is optimized to achieve the desired level of isolation between the antenna elements, as depicted in Figure 6. It is important to note that the maximum $r_2$ value that can be used to ensure that the semicircular slots do not overlap and maintain their circular shape is 1.28 mm. The curved geometry of the semi-circles helps to redirect the coupling effect away from the antenna elements, reducing the amount of energy that is coupled between them. The size, shape, and placement of the semi-circle slots can be optimized to achieve the desired level of isolation between the antenna elements. In this sense, the incorporation of semi-circular slots at the edges of the ground surface of the antenna elements has been observed to enhance the isolation values of the antenna, as depicted in Figure 7a.

The proposed MIMO antenna is fabricated on an RT/Duroid 5880 substrate with a dielectric constant of $\varepsilon_r$=2.2 and a loss tangent (tan$\delta$) of 0.009, and the overall dimension of the substrate is 25 x 25 x 0.787 mm$^3$. The computer simulation tool CST Microwave Studio employed for designing, simulating and optimizing the proposed antenna.

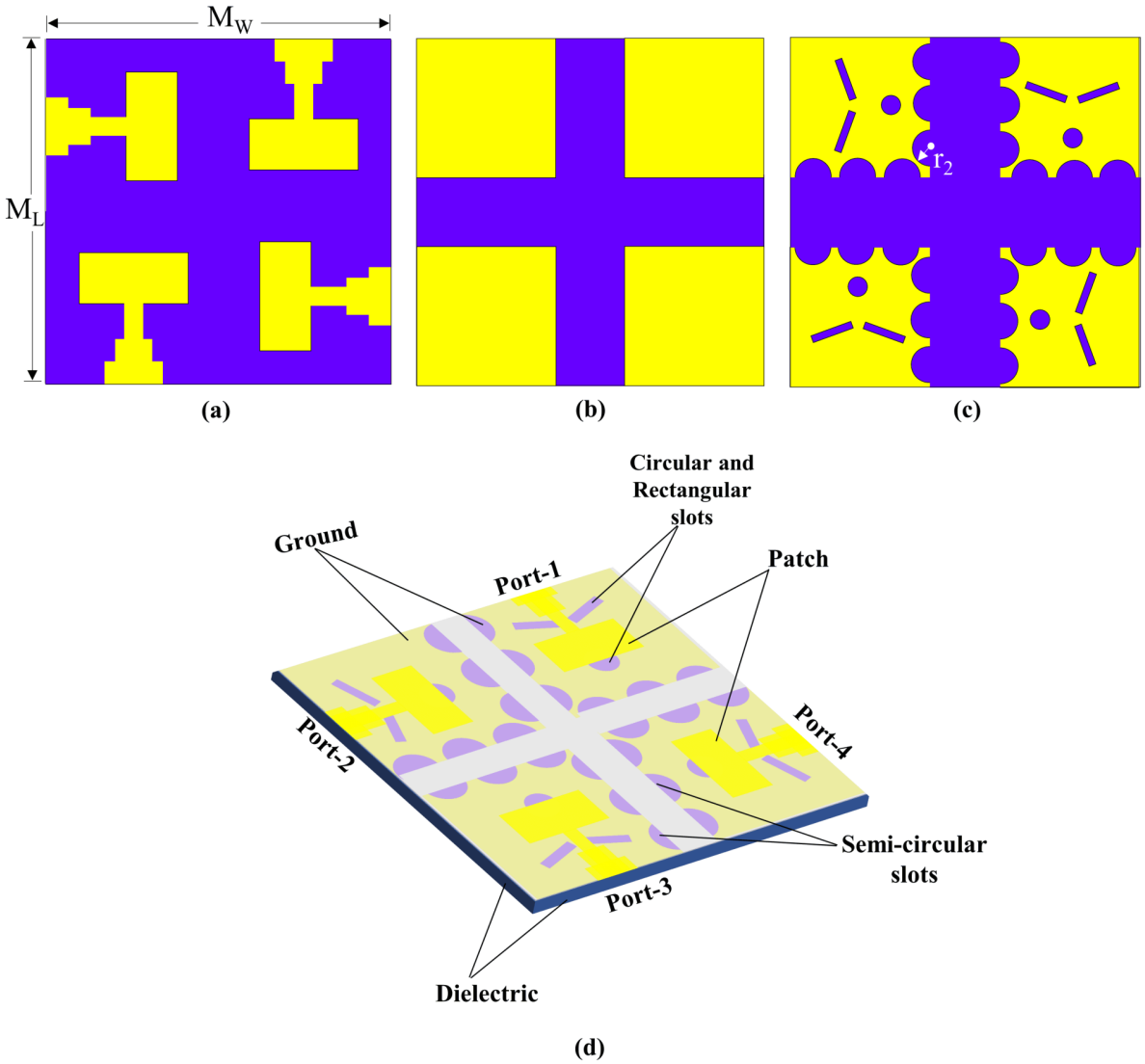


**Figure 5.** Design evolution of the proposed 4-port MIMO antenna, a) Top layer ($M_L$ = $M_W$ =25 mm), b) Bottom layer – Step I, c) Bottom layer – proposed, and d) 3D visualization of the physical structure of the proposed 4-port MIMO antenna.

Preprints (www.preprints.org) | NOT PEER-REVIEWED | Posted: 24 May 2023 doi:10.20944/preprints202305.1709.v1



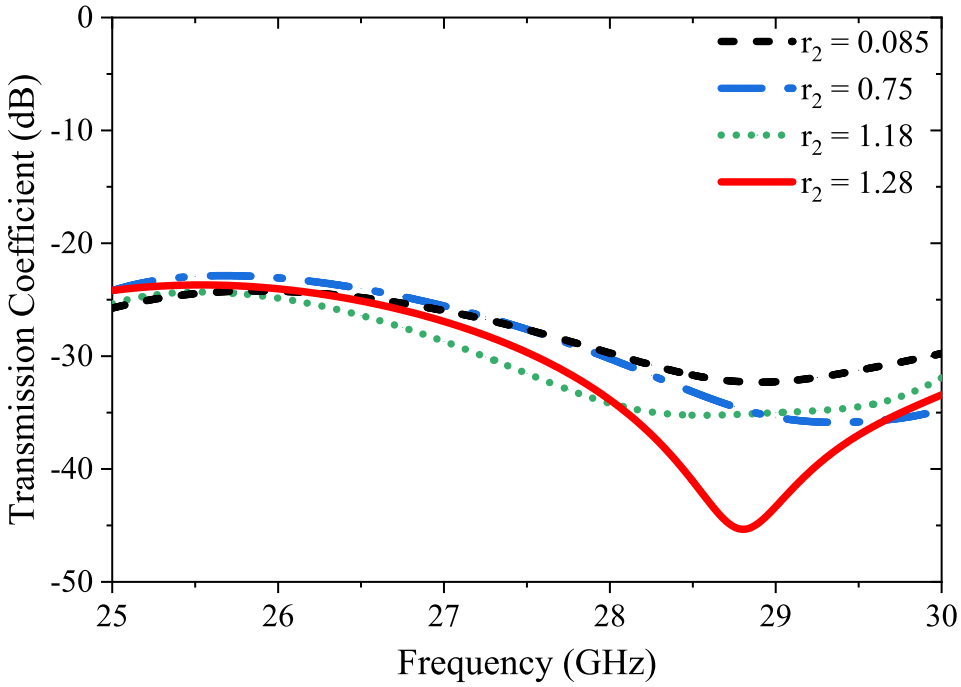


**Figure 6.** Parametric analysis of the diameter ($r_2$) of the semicircular slots.

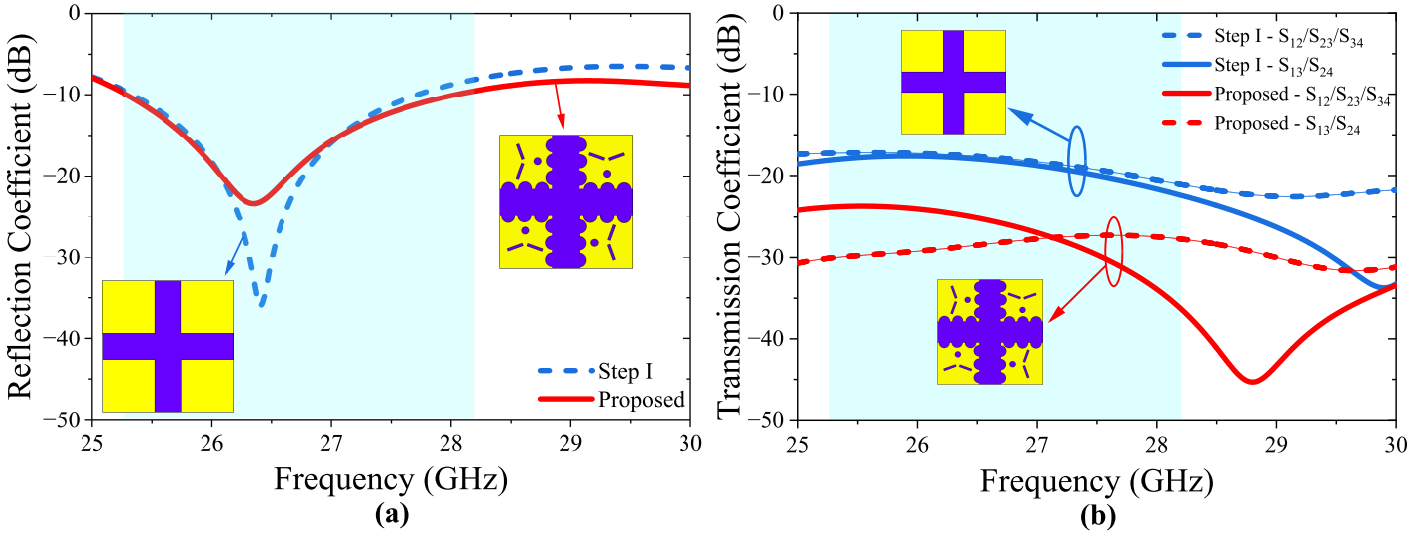


**Figure 7.** Reflection/Transmission coefficients of the proposed 4-port MIMO antenna.

As depicted in Figure 7, it can be observed that the incorporating of semi-circular slots along the edges of the ground surface of the antenna elements has resulted in a noteworthy improvement in isolation level of 13.6 dB. This is due to the fact that the semi-circular slots disturb the flow of the surface current distributions by diverting the conducting path that helps to reduce the coupling between antenna elements, resulting in a stronger isolation between the ports.

Preprints (www.preprints.org) | NOT PEER-REVIEWED | Posted: 24 May 2023 doi:10.20944/preprints202305.1709.v1



### 3. Results and Discussion

The proposed 4-port MIMO antenna is fabricated and measurement is tested using a network analyzer as shown in Figure 8a. The design is simulated using CST Microwave Studio software. A comparison between measured and simulated reflection/transmission coefficients is presented in Figure 8b,c. The slight difference between the simulation and the measurement results may have occurred due to the fabrication tolerances, SMA connector and coaxial cable losses.

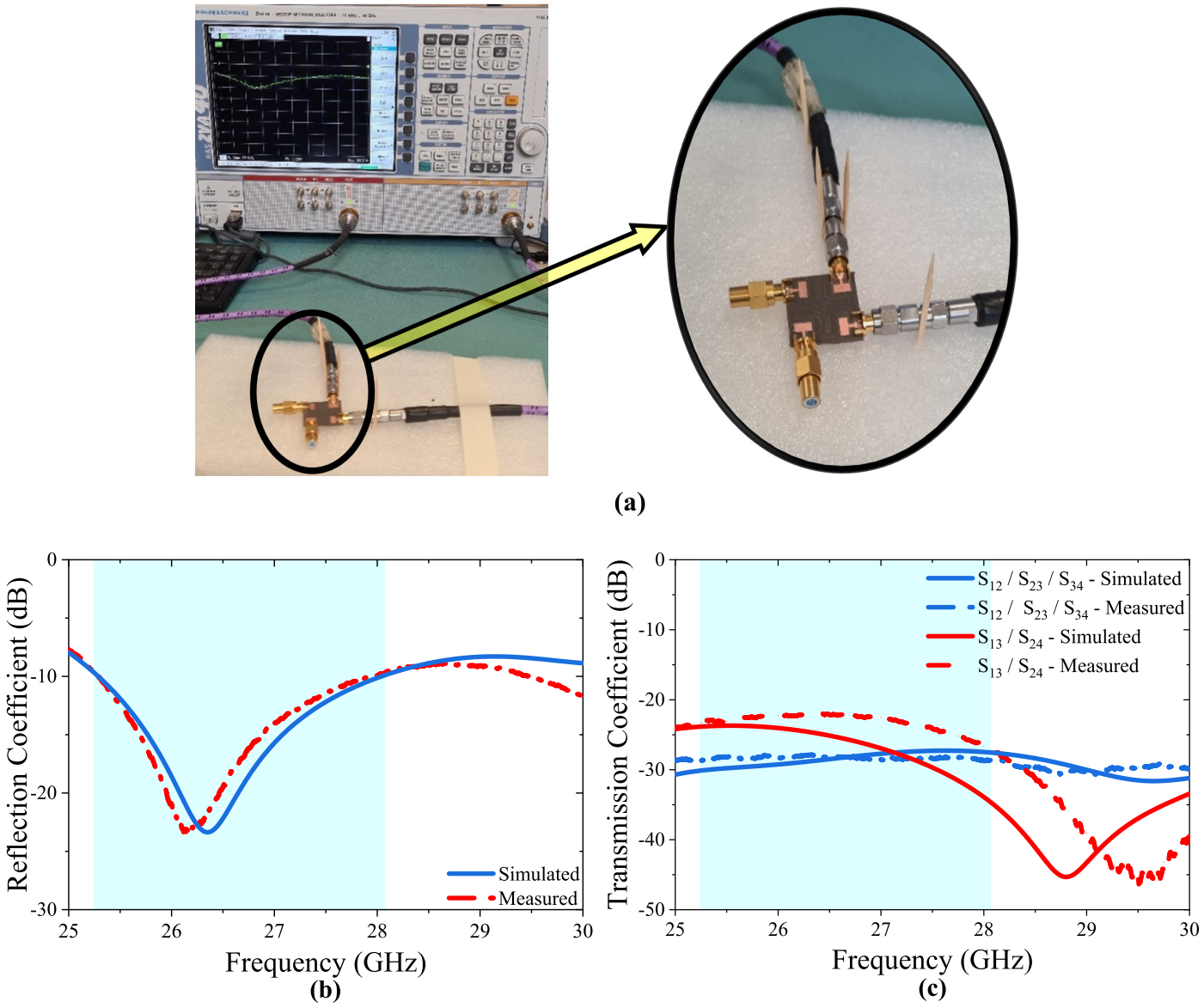


**Figure 8.** a) Measurement setup, b) Measured and simulated $S_{11}$ denotes the lowest $S_{11}$ of -23.5 dB between 25.28 GHz and 28.02 GHz, c) Measured transmission coefficients are obtained as minimum -29.4 dB for $S_{12}$ , $S_{13}$ , and -23.2 dB for $S_{13}$ and $S_{24}$ values.

Figure 9 illustrates the 3D radiation patterns of the proposed 4-port MIMO Antenna. As depicted in Figure 8a simulated peak gain within the desired frequency band is 8.72 dBi.

Preprints (www.preprints.org) | NOT PEER-REVIEWED | Posted: 24 May 2023 doi:10.20944/preprints202305.1709.v1



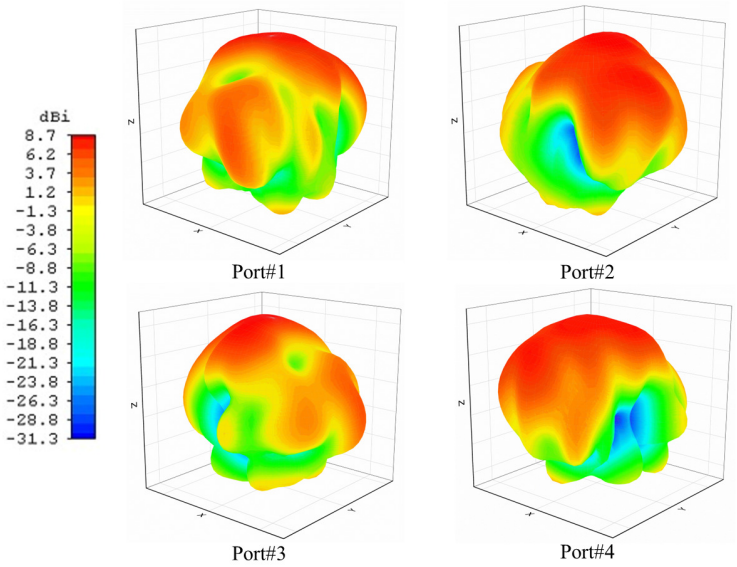


**Figure 9.** The 3D Directivity gain results of each antenna element in the presented MIMO Antenna.

Additionally, Figure 10 displays the surface current distribution plots for each antenna port, which show concentrated current distribution at the patch edges and slots drilled in the ground plane. The observation that the current distribution is higher on the patch surface where the circular and rectangular slots as DGS are located indicates that these slots have facilitated the propagation of electromagnetic waves, resulting in an improved bandwidth of the 4-port MIMO antenna. Each element has a maximum surface current amplitude of 160 A/m at a resonant frequency of 26.26 GHz In addition, the use of DGS, in the form of semi-circles placed at the edge of the ground plane, has contributed to the reduction of mutual coupling between the four orthogonally placed antenna elements, as observed in the Figure 10.

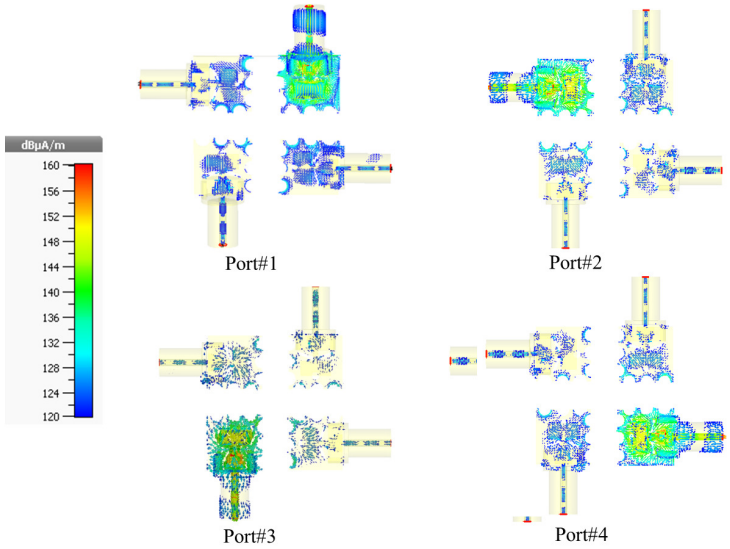


**Figure 10.** The surface current distribution of each antenna element.

The E and H planes are simulated at 26.26 GHz, and Figure 11 shows the Phi=0º H plane and Phi=90º E Plane for each antenna port. Both antennas have a wide edge radiation pattern with low side lobes in the E-plane. For port 1, the half-power beamwidth (HPBW) is 73.9º at Phi=0º and 46.5º at Phi=90º. For port 2, the HPBW is 46.6º at Phi=0º and 73.9º

Preprints (www.preprints.org) | NOT PEER-REVIEWED | Posted: 24 May 2023 doi:10.20944/preprints202305.1709.v1



at Phi=90°. For port 3, the HPBW is 73.9° at Phi=0° and 46.6° at Phi=90°. For port 4, the HPBW is 46.5° at Phi=0° and 73.9° at Phi=90°. As a result, the maximum radiation pattern is a parameter that is taken into consideration when evaluating the overall performance of the MIMO antenna.

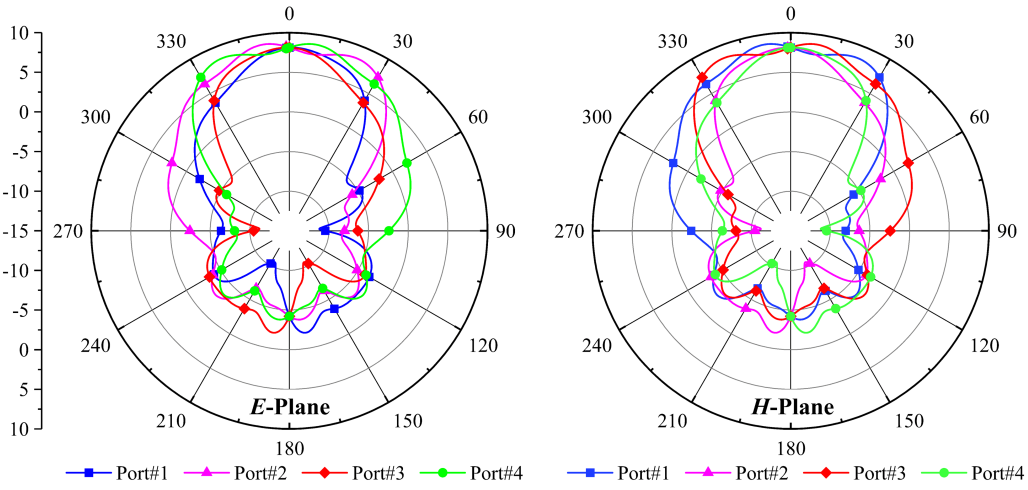


**Figure 11.** The E plane and H plane graphs superimposed for each port.

Envelope Correlation Coefficient (ECC) and Diversity Gain (DG), along with Total Active Reflection Coefficient (TARC), are metrics that provide crucial information about the antenna's ability to provide stable, high-quality, and diverse signals, thereby ensuring optimal system performance. Although MIMO antenna systems can theoretically increase a system's capacity, the system's performance can be negatively impacted if the signals received at different antenna elements are correlated [48]. ECC measures the degree of independence between the radiation patterns of two antennas. The theoretical assumption is that the ECC value should be zero in an ideal scenario where the antennas can radiate independently of each other. However, in practice, due to various losses, an ECC value of <0.5 is considered acceptable. This value indicates the little interaction between the antennas and determines how well the performance is. ECC can be expressed using the S parameters given in Equation (1) for any MIMO antenna system. In this study, the resulting ECC value of <0.0005 indicates a high degree of independence between the radiation patterns of the antennas and good performance, implying that the antennas are radiating independently of each other with very little interaction.

$$ECC = \frac{\left|S_{ii}^{*}S_{ij} + S_{ji}^{*}S_{jj}\right|^{2}}{\left(1 - |S_{ii}|^{2} - |S_{ji}|^{2}\right)\left(1 - |S_{jj}|^{2} - |S_{ij}|^{2}\right)} \quad (1)$$

Evaluating the adequacy of MIMO features involves considering Diversity Gain (DG) as another key component. Optimizing diversity gain is crucial for achieving a high-performance MIMO antenna system. If the envelope correlation coefficient (ECC) exceeds 0.5, the system fails to provide diversity gain, potentially degrading system performance. A value of $|ECC| \leq 0.3$ is considered sufficient to achieve diversity gain [49]. DG is derived from ECC using Equation (2) and measures the ability of antennas to reduce fading and improve the quality of the received signal in a multipath environment. The aim is to create an environment where the signals received by each antenna are as different as possible so that the receiver can combine them to improve the overall signal quality. DG is a crucial

Preprints (www.preprints.org) | NOT PEER-REVIEWED | Posted: 24 May 2023 doi:10.20944/preprints202305.1709.v1



factor in evaluating the performance of MIMO antennas as it is closely related to their ability to reduce fading and improve signal quality. Higher data rates and better system performance can be achieved by optimizing the diversity gain using Equation (2) to ensure a high diversity gain, typically around 10 dB [50].

$$DG = 10\sqrt{1 - |ECC|^2} \tag{2}$$

Figure 12 presents the results of the measured and simulated ECC and DG values for the proposed Multiple-Input Multiple-Output (MIMO) antenna.

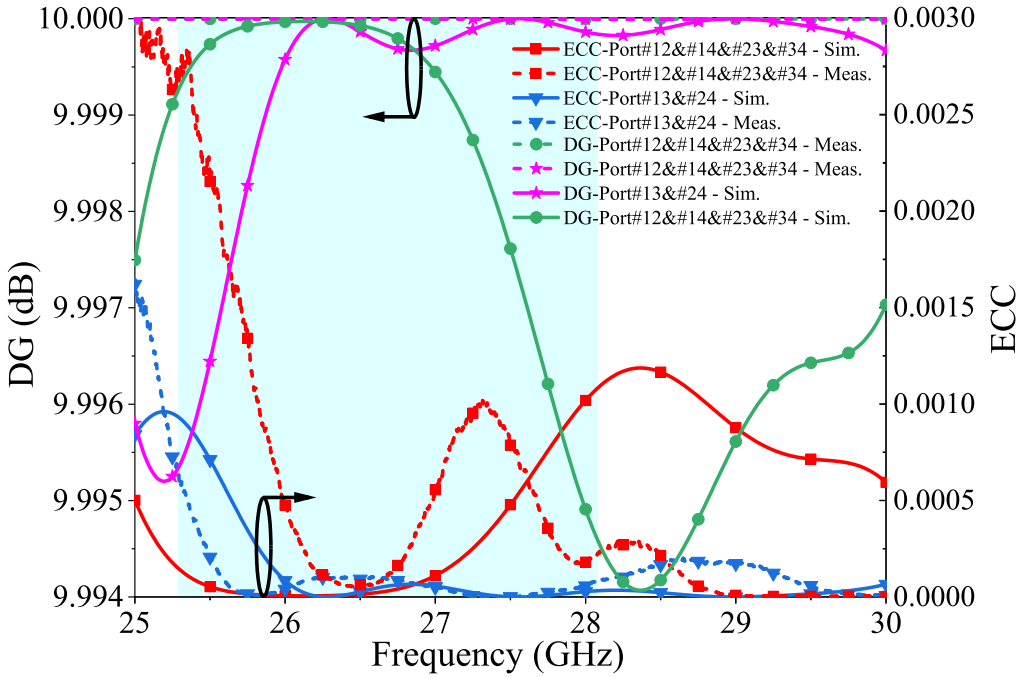


**Figure 12.** ECC and DG measured and simulated results of the proposed 4-port MIMO antenna.

The Total Active Reflection Coefficient (TARC) is an important parameter to consider when designing a MIMO communication system. TARC is calculated by taking the ratio of the square root of the total reflected power to the total power in the system, and is estimated by using arbitrary signal combinations and measuring excessive couplings between antenna ports. It is crucial that the TARC value does not exceed 0 dB, as this could lead to distorted received results and erroneous data transmission. Figure 13 shows the simulated and measured TARC values for the proposed 4-port MIMO antenna, which have been evaluated to be below 10 dB for most of the frequency range.

$$TARC = -\sqrt{\frac{(S_{11} + S_{12})^2 + (S_{21} + S_{22})^2}{2}} \tag{3}$$

Preprints (www.preprints.org) | NOT PEER-REVIEWED | Posted: 24 May 2023 doi:10.20944/preprints202305.1709.v1



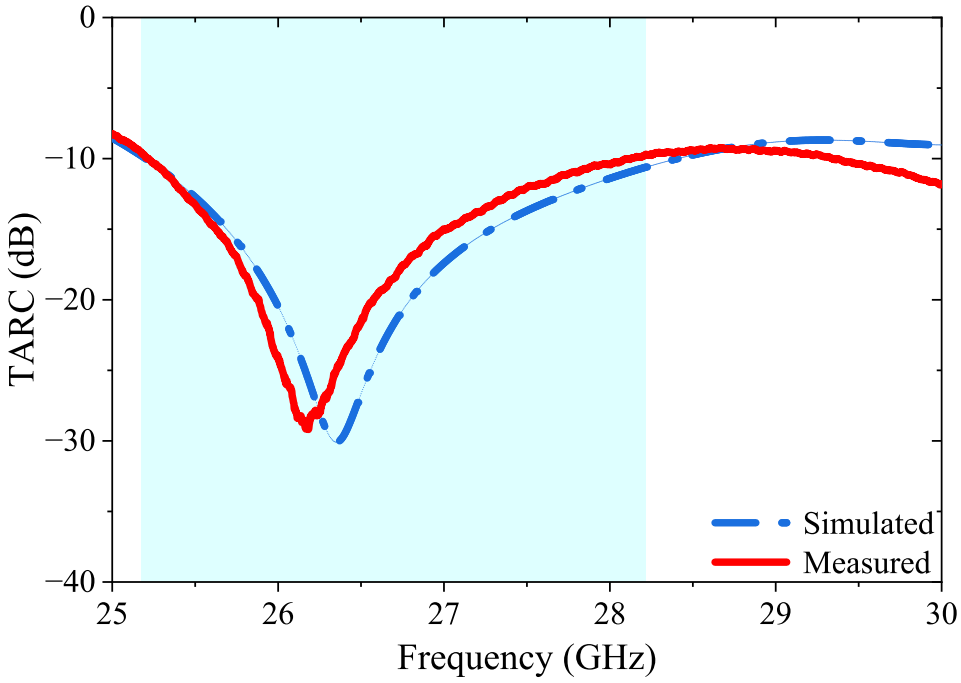


**Figure 13.** TARC measured and simulated results of the proposed 4-port MIMO antenna.

The Voltage Standing Wave Ratio (VSWR) is an essential metric that indicates the degree of impedance matching between the antenna and transmission line. It is defined as the ratio of the amplitudes of the forward and reflected waves along the transmission line. When the VSWR value is equal to 1, it signifies that all power is transferred to the antenna with no reflection, thereby ensuring optimal antenna performance. The simulated VSWR value of the antenna is 1.2; indicating that the impedance of the antenna matches the transmission line's impedance, allowing maximum power to be transferred from the source to the antenna.

Another critical metric in antenna design is directivity gain, which is the ratio of the radiation intensity of an antenna in a particular direction to the average radiation intensity of the antenna over all directions. Antennas with higher directivity gain are more efficient, allowing for better transmission of signals over longer distances or reception of weaker signals. Therefore, directivity gain is a key factor to consider when designing and optimizing antennas for various applications, particularly in wireless communication systems. Figure 14 depicts the VSWR and DG of the 4-port MIMO antenna.

Preprints (www.preprints.org) | NOT PEER-REVIEWED | Posted: 24 May 2023 doi:10.20944/preprints202305.1709.v1



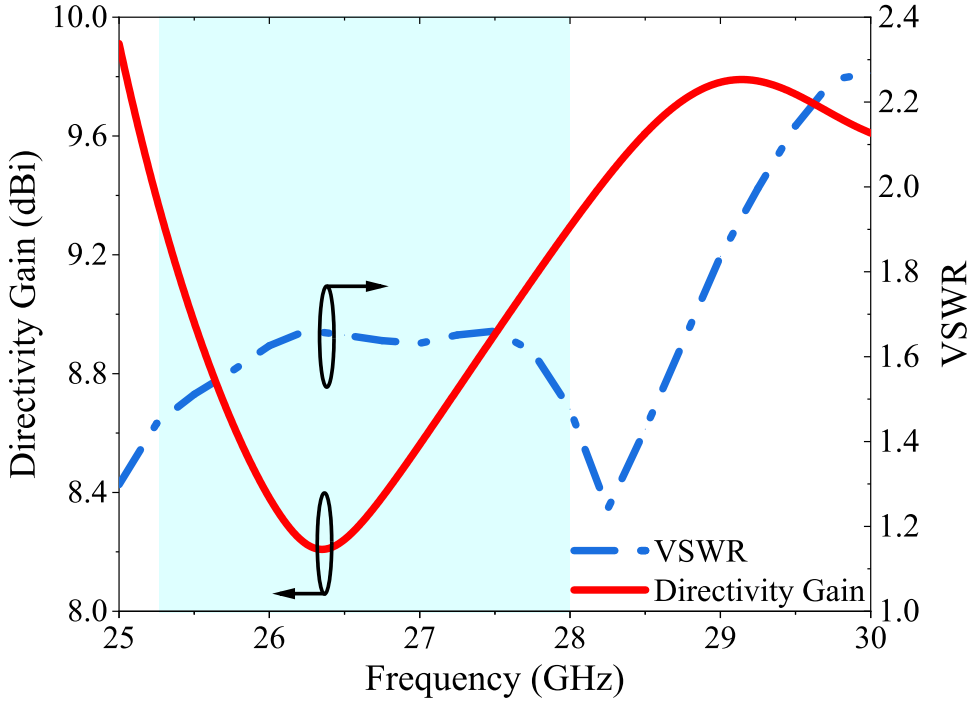


**Figure 14.** VSWR and DG results of the proposed 4-port MIMO antenna.

Table 2 presents a comparison of the proposed MIMO antenna with the recent published literature in terms of the method used for isolation, the operating frequency of system, the the number of ports in the MIMO antenna, the size of the MIMO antenna, the realized gain, the isolation levels between antenna elements and the Effective Channel Capacity. It is seen from the table, the antenna suggested in this manuscript has the lowest ECC values excluding designs investigated in [38–43]. Despite the ECC values provided in [38–43] being lower than those of the proposed antenna in the manuscript, Ref. [38] has lower Max. Gain and Min. Isolation values, and Ref. [43] has a higher volume antenna while having a Max. Gain value lower than the proposed antenna. Although the Max. Gain and Min. Isolation values of Ref. [35] are higher compared to the proposed antenna, it is observed that Ref. [35] has a complex design and a high volume structure, and the ECC value is lower than the proposed study. Furthermore, despite Ref. [43] exhibits lower Min. isolation and ECC values compared to the proposed antenna, Ref. [43] pertains to a high volume antenna, which results in a lower Max. Gain value compared to the proposed antenna.

 doi:10.20944/preprints202305.1709.v1



**Table 2.** Comparison of this study with other studies in terms of bandwidth, isolation, directivity gain and ECC.

| Ref. | Method Used for Isolation | Operating Frequency (GHz) | Design Complexity | Size ($\lambda_0$x$\lambda_0$x$\lambda_0$) | Min.Isolation (dB) | Max. Gain, (dBi) | ECC |
|---|---|---|---|---|---|---|---|
| [34] | DGS | 25.5-29.6 | High | 2.8x3.27x0.071 | 17 | 8.3 | <0.01 |
| [35] | PRS | 25-33 | High | 1.58x1.58x0.7 | 25 | 14.1 | <0.008 |
| [36] | PGS | 3-13.5 | Low | 0.73x0.73x0.279 | 15 | 3.5 | <0.4 |
| [37] | PGS + MS | 3.11-7.67 | High | 0.58x0.58x0.02 | 15.5 | 8.3 | <0.004 |
| [38] | DGS | 3.11-7.67 | Low | 4.48x1.12x0.02 | 20 | 11 | <0.005 |
| [39] | DGS | 27-29 | Low | 2.21x1.4x0.069 | 17 | 7.8 | <0.001 |
| [40] | DGS | 24.647-28.182 | Low | 2.65x2.47x0.044 | 22 | 6.22 | <0.05 |
| [41] | DGS | 23.3-32.1 | Low | 1.44x1.44x0.045 | 15 | <10 | <0.03 |
| [42] | DGS | 27.2-29.2 | Low | 2.8x2.8x0.148 | 29 | <7.1 | <0.0005 |
| [43] | O-DGS | 25-50 | Low | 3.33x3.33x0.023 | 20 | - | <0.005 |
| [44] | DGS | 24.8-27.6 | Low | 4.13x5.54x0.508 | 20 | 9 | <0.002 |
| [45] | Orientation | 2.42-2.48 | Low | 7.93x12.26x0.13 | 20 | 5.37 | <0.013 |
| [46] | DB | 2.9-10.86 | High | 1.3x1.3x0.002 | 22 | 4 | <0.01 |
| [47] | Stub | 2-10.6 | Low | 0.82x0.82x0.029 | 17 | 3 | <0.003 |
| **This Work** | **DGS** | **25.28-28.02** | **Low** | **2.21x2.21x0.069** | **23.2** | **8.72** | **<0.0015** |

## 4. Conclusions

In recents years, the 5G technology has emerged by its critical significance as a communication service. This is largely due to its ability to provide higher multi-Gbps peak data speeds, ultra-low latency, increased network capacity, heightened availability, greater reliability, and a more uniform user experience to a larger number of users. Besides, there is a growing trend towards the development of lighter and thinner portable gadgets that demand powerful processing capability. This manuscript presents a novel, compact and low-profile 4-port MIMO antenna design for millimeter-wave applications operating at 26.35 GHz. The antenna has dimensions of 25250.787 $mm^3$ and is built on a relatively small, low-cost substrate of RT/Duroid 5880. It is suitable for use over a wide frequency band of 25.28-28.02 GHz, achieving a minimum isolation value of 23.2 dB and a directivity gain of 8.72 dBi. MIMO metrics such as ECC, DG, and CCL were simulated and calculated from measured data to verify the diversity performance of the proposed antenna and demonstrate its superior characteristics. The proposed MIMO antenna is distinct from other reported works in the literature with its wide operating bandwidth, high isolation, low ECC, design features, compact size, and low cost. Due to these characteristics, it has great potential for use in a wide range of 5G applications.

**Author Contributions:** These authors contributed equally to this work.

**Funding:** This research received no external funding.

**Institutional Review Board Statement:** Not applicable.

**Informed Consent Statement:** Not applicable.

**Data Availability Statement:** Not applicable.

**Conflicts of Interest:** The authors declare no conflict of interest.

## Abbreviations

The following abbreviations are used in this manuscript:

| | |
|---|---|
| DGS | Defected Ground Structure |
| PRS | Partially Reflecting Surface |
| DPE | Diagonal Parasitic Element |
| PGS | Partial Ground Surface |
| MS | Metasurface |
| O-DGS | Orientation-DGS |
| DB | Decoupling Branches |

DG - Diversity Gain

## References


1. Jhunjhunwala, V.K.; Ali, T.; Kumar, P.; Kumar, P.; Kumar, P.; Shrivastava, S.; Bhagwat, A.A. Flexible UWB and MIMO antennas for wireless body area network: A review. *Sensors (Basel, Switzerland)* **2022**, *22*, 9549. https://doi.org/10.3390/s22239549.
2. Anchidin, L.; Lavric, A.; Mutescu, P.M.; Petrariu, A.I.; Popa, V. The design and development of a microstrip antenna for Internet of Things applications. *Sensors (Basel, Switzerland)* **2023**, *23*, 1062. https://doi.org/10.3390/s23031062.
3. Sgora, A. 5G spectrum and regulatory policy in Europe: An overview. In Proceedings of the 2018 Global Information Infrastructure and Networking Symposium (GIIS). IEEE, 2018.
4. Chettri, L.; Bera, R. A comprehensive survey on internet of things (IoT) toward 5G wireless systems. *IEEE internet of things journal* **2020**, *7*, 16–32. https://doi.org/10.1109/jiot.2019.2948888.
5. Biswas, S.; Sanyal, A.; Božanić, D.; Puška, A.; Marinković, D. Critical success factors for 5G technology adaptation in supply chains. *Sustainability* **2023**, *15*, 5539. https://doi.org/10.3390/su15065539.
6. Umoh, V.; Ekpe, U.; Davidson, I.; Akpan, J. Mobile broadband adoption, performance measurements and methodology: A review. *Electronics* **2023**, *12*, 1630. https://doi.org/10.3390/electronics12071630.
7. Soos, G.; Ficzere, D.; Varga, P. Towards traffic identification and modeling for 5G application use-cases. *Electronics* **2020**, *9*, 640. https://doi.org/10.3390/electronics9040640.
8. Peralta-Ochoa, A.M.; Chaca-Asmal, P.A.; Guerrero-Vásquez, L.F.; Ordoñez-Ordoñez, J.O.; Coronel-González, E.J. Smart healthcare applications over 5G networks: A systematic review. *Applied sciences (Basel, Switzerland)* **2023**, *13*, 1469. https://doi.org/10.3390/app13031469.
9. Al-Ogaili, F.; Shubair, R.M. Millimeter-wave mobile communications for 5G: Challenges and opportunities. In Proceedings of the 2016 IEEE International Symposium on Antennas and Propagation (APSURSI). IEEE, 2016.
10. Heath, R.W.; Gonzalez-Prelcic, N.; Rangan, S.; Roh, W.; Sayeed, A.M. An overview of signal processing techniques for millimeter wave MIMO systems. *IEEE journal of selected topics in signal processing* **2016**, *10*, 436–453. https://doi.org/10.1109/jstsp.2016.2523924.
11. Sun, S.; Rappaport, T.; Heath, R.; Nix, A.; Rangan, S. Mimo for millimeter-wave wireless communications: beamforming, spatial multiplexing, or both? *IEEE communications magazine* **2014**, *52*, 110–121. https://doi.org/10.1109/mcom.2014.6979962.
12. Kumaravelu, V.B.; Jaiswal, G.; Gudla, V.V.; Ramachandra Reddy, G.; Murugadass, A. Modified spatial modulation: An alternate to spatial multiplexing for 5G-based compact wireless devices. *Arabian journal for science and engineering* **2019**, *44*, 6693–6709. https://doi.org/10.1007/s13369-018-3572-9.
13. Sanguinetti, L.; Bjornson, E.; Hoydis, J. Toward massive MIMO 2.0: Understanding spatial correlation, interference suppression, and pilot contamination. *IEEE transactions on communications* **2020**, *68*, 232–257. https://doi.org/10.1109/tcomm.2019.2945792.
14. Alharbi, A.G.; Rafique, U.; Ullah, S.; Khan, S.; Abbas, S.M.; Ali, E.M.; Alibakhshikenari, M.; Dalarsson, M. Novel MIMO antenna system for ultra wideband applications. *Applied sciences (Basel, Switzerland)* **2022**, *12*, 3684. https://doi.org/10.3390/app12073684.
15. Sheriff, N.; Kamal Abdul Rahim, S.; Tariq Chattha, H.; Kim Geok, T. Multiport single element Mimo antenna systems: A review. *Sensors (Basel, Switzerland)* **2023**, *23*. https://doi.org/10.3390/s23020747.
16. Alibakhshikenari, M.; Babaeian, F.; Virdee, B.S.; Aissa, S.; Azpilicueta, L.; See, C.H.; Althuwayb, A.A.; Huynen, I.; Abd-Alhameed, R.A.; Falcone, F.; et al. A comprehensive survey on "various decoupling mechanisms with focus on metamaterial and metasurface principles applicable to SAR and MIMO antenna systems". *IEEE access: practical innovations, open solutions* **2020**, *8*, 192965–193004. https://doi.org/10.1109/access.2020.3032826.
17. Kumar, A.; Ansari, A.Q.; Kanaujia, B.K.; Kishor, J.; Matekovits, L. A review on different techniques of mutual coupling reduction between elements of any MIMO antenna. Part 2: Metamaterials and many more. *Radio science* **2021**, *56*. https://doi.org/10.1029/2020rs007222.
18. Thi Thanh Tu, D.; Gia Thang, N.; Tuan Ngoc, N.; Thi Bich Phuong, N.; Van Yem, V. 28/38 GHz dual-band MIMO antenna with low mutual coupling using novel round patch EBG cell for 5G applications. In Proceedings of the 2017 International Conference on Advanced Technologies for Communications (ATC). IEEE, 2017.
19. Ahmad, I.; Tan, W.; Ali, Q.; Sun, H. Latest performance improvement strategies and techniques used in 5G antenna designing technology, a comprehensive study. *Micromachines* **2022**, *13*, 717. https://doi.org/10.3390/mi13050717.

20. Kapure, V.R.; Rathod, S.S. A two element EBG-inspired UWB MIMO antenna with triple band notched characteristics and high isolation. *Sadhana* **2023**, *48*. https://doi.org/10.1007/s12046-022-02055-2.
21. Babu, N.S.; Ansari, A.Q.; Kanaujia, B.K.; Singh, G.; Kumar, S. A two-port UWB MIMO antenna with an EBG structure for WLAN/ISM applications. *Materials today: proceedings* **2023**, *74*, 334–339. https://doi.org/10.1016/j.matpr.2022.08.316.
22. Islam, H.; Das, S.; Ali, T.; Bose, T.; Prakash, O.; Kumar, P. A frequency reconfigurable MIMO antenna with bandstop filter decoupling network for cognitive communication. *Sensors (Basel, Switzerland)* **2022**, *22*, 6937. https://doi.org/10.3390/s22186937.
23. Amin, F.; Saleem, R.; Shabbir, T.; Rehman, S.u.; Bilal, M.; Shafique, M.F. A compact quad-element UWB-MIMO antenna system with parasitic decoupling mechanism. *Applied sciences (Basel, Switzerland)* **2019**, *9*, 2371. https://doi.org/10.3390/app9112371.
24. Liu, Y.; Yang, Z.; Chen, P.; Xiao, J.; Ye, Q. Isolation enhancement of a two-monopole MIMO antenna array with various parasitic elements for sub-6 GHz applications. *Micromachines* **2022**, *13*, 2123. https://doi.org/10.3390/mi13122123.
25. Wu, A.; Tao, Y.; Zhang, P.; Zhang, Z.; Fang, Z. A compact high-isolation four-element MIMO antenna with asymptote-shaped structure. *Sensors (Basel, Switzerland)* **2023**, *23*. https://doi.org/10.3390/s23052484.
26. Yon, H.; Rahman, N.H.A.; Aris, M.A.; Jamaluddin, M.H.; Kong Cheh Lin, I.; Jumaat, H.; Mohd Redzwan, F.N.; Yamada, Y. Development of C-shaped parasitic MIMO antennas for mutual coupling reduction. *Electronics* **2021**, *10*, 2431. https://doi.org/10.3390/electronics10192431.
27. Kumar, P.; Ali, T.; Mm, M.P. Characteristic mode analysis-based compact dual band-notched UWB MIMO antenna loaded with neutralization line. *Micromachines* **2022**, *13*. https://doi.org/10.3390/mi13101599.
28. Tiwari, R.N.; Singh, P.; Kanaujia, B.K.; Srivastava, K. Neutralization technique based two and four port high isolation MIMO antennas for UWB communication. *Archiv fur Elektronik und Ubertragungstechnik [International journal of electronics and communications]* **2019**, *110*, 152828. https://doi.org/10.1016/j.aeue.2019.152828.
29. Sandi, E.; Diamah, A.; Permata Putri, R.A. Combination of EBG and DGS to improve MIMO antenna isolation. In Proceedings of the 2022 IEEE International Conference on Aerospace Electronics and Remote Sensing Technology (ICARES). IEEE, 2022.
30. Li, Y.; Bian, L.A.; Xu, K.d.; Liu, Y.; Wang, Y.; Chen, R.; Xie, S. Mutual coupling reduction for monopole MIMO antenna using l-shaped stubs, defective ground and chip resistors. *Archiv fur Elektronik und Ubertragungstechnik [International journal of electronics and communications]* **2023**, *160*, 154524. https://doi.org/10.1016/j.aeue.2022.154524.
31. Ameen, M.; Chaudhary, R.K. Isolation enhancement of metamaterial-inspired two-port MIMO antenna using hybrid techniques. *IEEE transactions on circuits and systems. II, Express briefs: a publication of the IEEE Circuits and Systems Society* **2023**, p. 1–1. https://doi.org/10.1109/tcsii.2023.3237831.
32. Paiva, S.B.; Junior, A.G.D.; Neto, V.P.S.; D'Assunção, A.G. A new compact dual-polarized MIMO antenna using slot and parasitic element decoupling for 5G and WLAN applications. *Electronics* **2022**, *11*, 1943. https://doi.org/10.3390/electronics11131943.
33. Althuwayb, A.A. Low-interacted multiple antenna systems based on metasurface-inspired isolation approach for MIMO applications. *Arabian journal for science and engineering* **2022**, *47*, 2629–2638. https://doi.org/10.1007/s13369-021-05720-6.
34. Khalid, M.; Iffat Naqvi, S.; Hussain, N.; Rahman, M.; Fawad.; Mirjavadi, S.S.; Khan, M.J.; Amin, Y. 4-port MIMO antenna with defected ground structure for 5G millimeter wave applications. *Electronics* **2020**, *9*, 71. https://doi.org/10.3390/electronics9010071.
35. Hussain, N.; Jeong, M.J.; Park, J.; Kim, N. A broadband circularly polarized Fabry-Perot resonant antenna using A single-layered PRS for 5G MIMO applications. *IEEE access: practical innovations, open solutions* **2019**, *7*, 42897–42907. https://doi.org/10.1109/access.2019.2908441.
36. Khan, A.A.; Naqvi, S.A.; Khan, M.S.; Ijaz, B. Quad port miniaturized MIMO antenna for UWB 11 GHz and 13 GHz frequency bands. *Archiv fur Elektronik und Ubertragungstechnik [International journal of electronics and communications]* **2021**, *131*, 153618. https://doi.org/10.1016/j.aeue.2021.153618.
37. Hasan, M.M.; Islam, M.T.; Samsuzzaman, M.; Baharuddin, M.H.; Soliman, M.S.; Alzamil, A.; Abu Sulayman, I.I.M.; Islam, M.S. Gain and isolation enhancement of a wideband MIMO antenna using metasurface for 5G sub-6 GHz communication systems. *Scientific reports* **2022**, *12*, 9433. https://doi.org/10.1038/s41598-022-13522-5.
38. Munir, M.E.; Kiani, S.H.; Savci, H.S.; Marey, M.; Khan, J.; Mostafa, H.; Parchin, N.O. A four element mm-wave MIMO antenna system with wide-band and high isolation characteristics for 5G applications. *Micromachines* **2023**, *14*, 776. https://doi.org/10.3390/mi14040776.
39. Rahman, S.; Ren, X.C.; Altaf, A.; Irfan, M.; Abdullah, M.; Muhammad, F.; Anjum, M.R.; Mursal, S.N.F.; AlKahtani, F.S. Nature inspired MIMO antenna system for future mmWave technologies. *Micromachines* **2020**, *11*, 1083. https://doi.org/10.3390/mi11121083.
40. Khalid, H.; Khalid, M.; Fatima, A.; Khalid, N. $2 \times 2$ MIMO antenna with defected ground structure for mm-wave 5G applications. In Proceedings of the 2019 13th International Conference on Mathematics, Actuarial Science, Computer Science and Statistics (MACS). IEEE, 2019.
41. Shah, S.T.; Shakir, S.; Durani, M.H.; Ahmed, U.; Bilal, M. Miniaturized four port MIMO antenna system for 5G mm-wave applications. In Proceedings of the 2021 1st International Conference on Microwave, Antennas and Circuits (ICMAC). IEEE, 2021.
42. Hussain, M.; Mousa Ali, E.; Jarchavi, S.M.R.; Zaidi, A.; Najam, A.I.; Alotaibi, A.A.; Althobaiti, A.; Ghoneim, S.S.M. Design and characterization of compact broadband antenna and its MIMO configuration for 28 GHz 5G applications. *Electronics* **2022**, *11*, 523. https://doi.org/10.3390/electronics11040523.

43. Abbas, M.A.; Allam, A.; Gaafar, A.; Elhennawy, H.M.; Sree, M.F.A. Compact UWB MIMO antenna for 5G millimeter-wave applications. *Sensors (Basel, Switzerland)* **2023**, *23*. https://doi.org/10.3390/s23052702.
44. Abdel Fat, S.Y.; Hamad, E.K.I.; Swelam, W.; Allam, A.M.; Mohamed, H.A.E. Design of compact 4-port Mimo antenna based on minkowski fractal shape dgs for 5g applications. *Progress in electromagnetics research C. Pier C* **2021**, *113*, 123–136. https://doi.org/10.2528/pierc21042703.
45. Abdulkawi, W.M.; Alqaisei, M.A.; Sheta, A.F.A.; Elshafiey, I. New compact antenna array for MIMO Internet of Things applications. *Micromachines* **2022**, *13*, 1481. https://doi.org/10.3390/mi13091481.
46. Zhang, J.; Du, C.; Wang, R. Design of a four-port flexible UWB-MIMO antenna with high isolation for wearable and IoT applications. *Micromachines* **2022**, *13*, 2141. https://doi.org/10.3390/mi13122141.
47. Tripathi, S.; Mohan, A.; Yadav, S. A compact Koch fractal UWB MIMO antenna with WLAN band-rejection. *IEEE antennas and wireless propagation letters* **2015**, *14*, 1565–1568. https://doi.org/10.1109/lawp.2015.2412659.
48. Hassan, M.M.; Rasool, M.; Asghar, M.U.; Zahid, Z.; Khan, A.A.; Rashid, I.; Rauf, A.; Bhatti, F.A. A novel UWB MIMO antenna array with band notch characteristics using parasitic decoupler. *Journal of electromagnetic waves and applications* **2020**, *34*, 1225–1238. https://doi.org/10.1080/09205071.2019.1682063.
49. Abdulkawi, W.M.; Malik, W.A.; Rehman, S.U.; Aziz, A.; Sheta, A.F.A.; Alkanhal, M.A. Design of a compact dual-band MIMO antenna system with high-diversity gain performance in both frequency bands. *Micromachines* **2021**, *12*, 383. https://doi.org/10.3390/mi12040383.
50. Liu, Y.; Yang, X.; Jia, Y.; Guo, Y.J. A low correlation and mutual coupling MIMO antenna. *IEEE access: practical innovations, open solutions* **2019**, *7*, 127384–127392. https://doi.org/10.1109/access.2019.2939270.